

**The structural basis of actinomycin D binding induces nucleotide
flipping-out, a sharp bend and a left-handed twist in CGG triplet
repeats**

Yu-Sheng Lo^{1†}, Wen-Hsuan Tseng^{1†}, Chien-Ying Chuang¹, and
Ming-Hon Hou^{1,2,3}

Supporting Information

Figure legends for supporting information

Figure S1. A refined ($2F_o - F_c$) Fourier electron density map showing the five amino acids (threonine, N-methylvaline, sarcosine, proline, and D-valine).

Figure S2. Schematic diagram of the ActD-(ATGCGGCAT)₂ as observed in the crystal structure.

Figure S3. Molecular interactions due to crystal packing. The flipped-out G6 (**A**) and G15 (**B**) bases of the DNA duplex form hydrogen bonds and mutual stacking interaction with the flipped out G6 and G15 bases of other duplexes with an equivalent symmetry.

Figure S4. The detailed conformation showing the stacking interactions in the ActD1-DNA (left) and ActD2-DNA (right) complexes at various base pair steps of the refined structure viewed from the minor groove direction. Hydrogen bonds are indicated as blue dotted lines.

Figure S5. Superimposition of the crystal structures of ActD1 (blue), ActD2 (green), and free ActD (red).

Figure S6. Comparison of the DNA twist (**A**), roll (**B**) and tilt (**C**) parameters in the structure of the ActD-(ATGCGGCAT)₂ complex. Typical values for A-DNA (solid line) and B-DNA (dashed line) are also shown.

Figure S7. (A) The crystal packing (P6₅22) diagram of the ActD-DNA complex. (B) Two major different packing interactions occur between the two asymmetric units in the crystal lattice (P6₅22): end-to-end and end-to-side, mediated by π - π stacking, and van der Waals contact.

Figure S8. Sensorgram of the ActD-DNA interaction between immobilised hairpin DNA duplexes including GG2 (A), AT2 (B), and GC2 (C), and the target ActD at various concentrations (2, 1, 0.75, 0.5, and 0.25 μ M from top to bottom) in 50 mM NaCl buffered with 20 mM Tris-HCl buffer at pH 7.3. The sensorgram was obtained by subtracting the reference control. The black lines represent the fitted curves.

Figure S9. A schematic illustration of the binding of ActD to the (CGG)₁₆ sequence is shown.

Table SI. Crystallographic and Refinement Data of ATGCGGCA[br⁵U]- Actinomycin D Complex.

λ for data collection (Å)	0.9062	0.9195	0.9189	0.8563
		Inflection point	peak	high remote
<i>Crystallographic data</i>				
$a=b$ (Å)	86.93	87.07	87.09	87.08
c (Å)	49.78	49.90	49.09	49.90
Space group			P6 ₅ 22	
Resolution (Å)	30-2.6	50-2.8	50-2.8	50-2.8
# reflections (>0 $\sigma(I)$)	48854	35451	38138	35367
$\langle I/\sigma(I) \rangle$	27.0	37.1	20.5	36.1
R _{merge} (%)	9.7	7.7	6.9	7.8
Completeness (%)	99.8	99.5	99.6	99.5
<i>Refinement data</i>				
R-factor/R-free (5% data)	0.26/0.29			
r.m.s.d. (Å)	0.004			
r.m.s.d. (°)	1.40			
# of DNA atoms	366			
# of drug atoms	179			
# of waters	133			
*Including Friedel's pairs				

Table SII. Base pair parameters for the ActD-(ATGCGGCAT)₂ complex.

Local base-pair parameters						
bp	Shear (Å)	Stretch (Å)	Stagger (Å)	Buckle (°)	Propeller (°)	Opening (°)
A1-T18	-1.26	0.17	0.51	-3.39	-13.36	8.51
T2-A17	-0.34	-0.17	0.55	-11.87	-17.21	0.73
G3-C16	-0.41	-0.36	0.97	7.55	18.33	1.21
C4+G14	-0.57	2.76	0.87	4.06	28.70	-120.37
G5-C13	-0.29	-0.24	0.52	5.02	11.40	-16.18
C7-G12	-0.43	-0.07	-0.84	14.84	22.04	-3.99
A8-T11	-0.08	0.54	1.01	39.48	-21.43	11.35
T9-A10	-1.31	-0.47	0.87	29.22	-17.37	7.00

Local base-pair parameters						
step	Shift (Å)	Slide (Å)	Rise (Å)	Tilt (°)	Roll (°)	Twist (°)
AT/AT	-0.95	-0.33	3.55	1.55	-13.23	32.94
TG/CA	1.01	2.00	3.38	-5.84	3.92	35.05
GC/GC	0.43	0.89	8.21	2.59	10.37	62.47
CG/CG	0.61	3.13	2.95	14.56	21.32	-43.45
GC/GC	0.80	2.94	6.68	11.52	10.20	5.84
CA/TG	0.12	1.92	2.98	-1.54	-1.17	35.43
AT/AT	0.69	-1.31	3.25	-4.43	0.89	31.70

Table SIII. Nucleic acid backbone torsion angles obtained for the ActD-(ATGCGGCAT)₂ complex.

Strand I								
Base	α	β	γ	δ	ϵ	ξ	χ	Puckering
A-1	----	----	51.7	146.9	-159.1	-97.6	-102.5	C2'-endo
T-2	-105.7	78.3	163.0	144.1	-121.8	-47.6	-166.2	C2'-endo
G-3	-76.6	163.5	31.1	138.1	-156.8	-128.7	-70.7	C2'-endo
C-4	-85.9	-140.4	34.4	139.4	176.1	-117.2	-58.5	C2'-endo
G-5	-53.2	-169.8	41.5	141.8	-157.5	-115.6	-58.9	C2'-endo
G-6	58.7	142.7	-50.8	162.3	-90.3	102.4	-100.6	C3'-exo
C-7	-118.0	175.1	46.5	145.2	-83.1	118.4	-83.7	C2'-endo
A-8	119.3	-113.4	149.5	145.0	-157.9	-109.2	-95.3	C2'-endo
T-9	34.2	-147.6	-85.5	142.6	----	----	-121.3	C2'-endo
Strand II								
Base	α	β	γ	δ	ϵ	ξ	χ	Puckering
T-18	-104.1	67.3	171.4	148.2	----	----	-155.6	C2'-endo
A-17	-60.7	128.2	51.4	150.4	-164.8	-75.2	-86.0	C2'-endo
C-16	101.1	-143.2	176.6	131.9	-80.6	-149.6	-162.9	C2'-endo
G-15	-47.1	174.6	46.3	148.4	-109.6	78.6	-112.3	C2'-endo
G-14	-18.2	-140.8	-50.1	153.0	-133.7	-87.8	108.0	C3'-exo
C-13	-57.1	-111.7	-58.1	149.1	-163.3	-94.7	-58.6	C3'-exo
G-12	-76.9	-168.3	51.9	144.3	-131.5	-82.5	-82.2	C2'-endo
T-11	56.3	144.4	-54.5	142.8	-177.6	-93.3	-105.1	C2'-endo
A-10	----	----	59.3	151.0	-172.7	-120.3	-143.4	C3'-exo

Figure S1

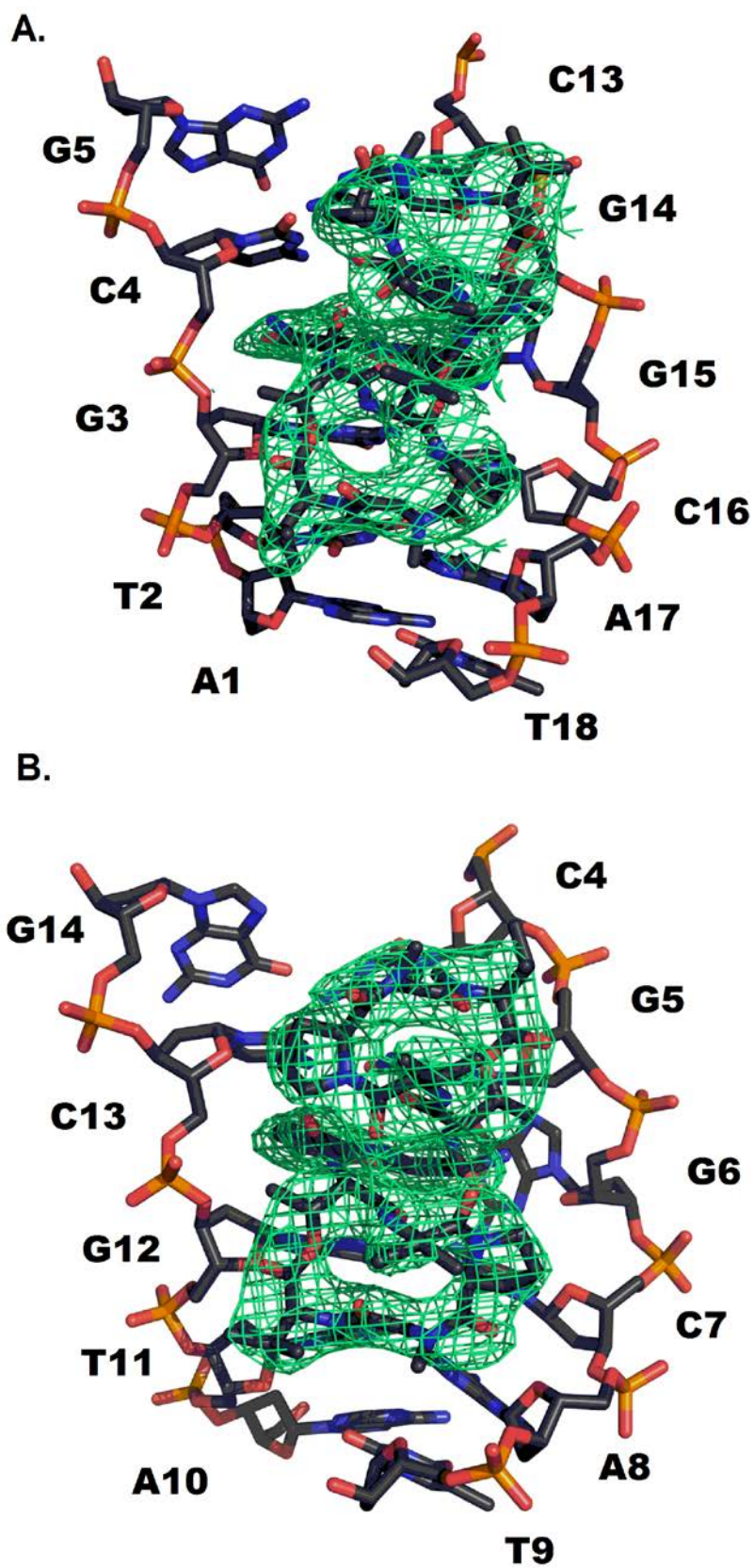


Figure S2

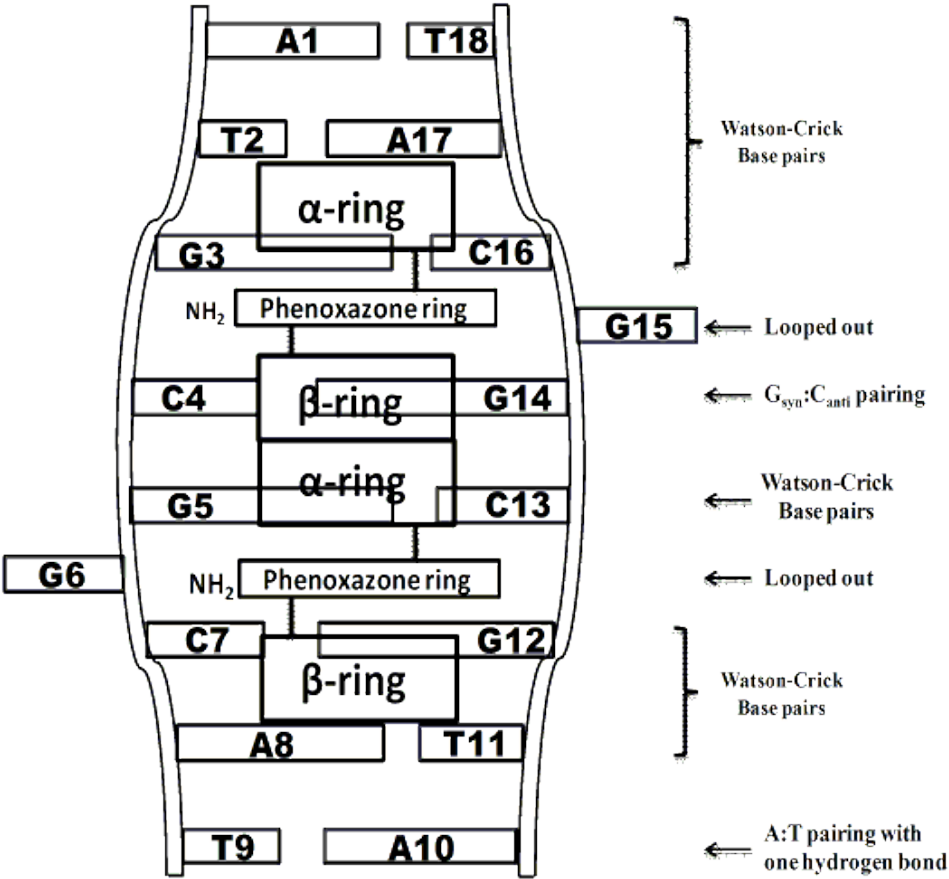
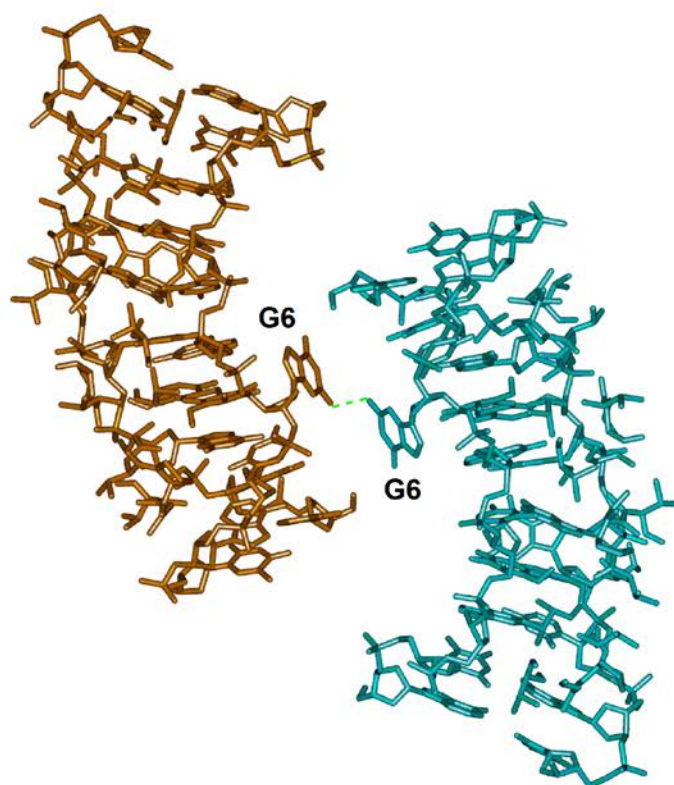


Figure S3

A.



B.

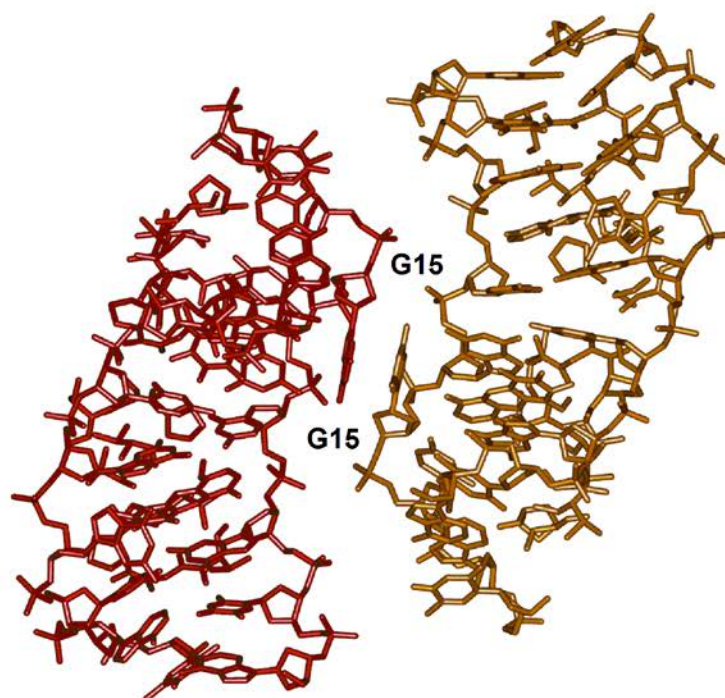
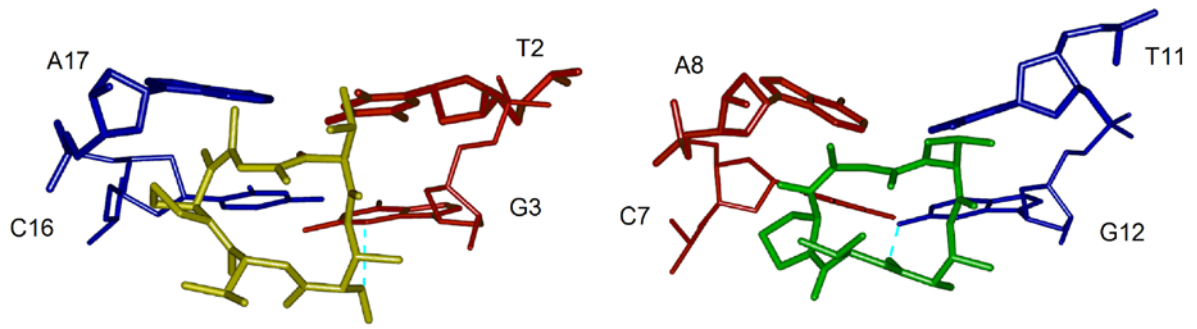
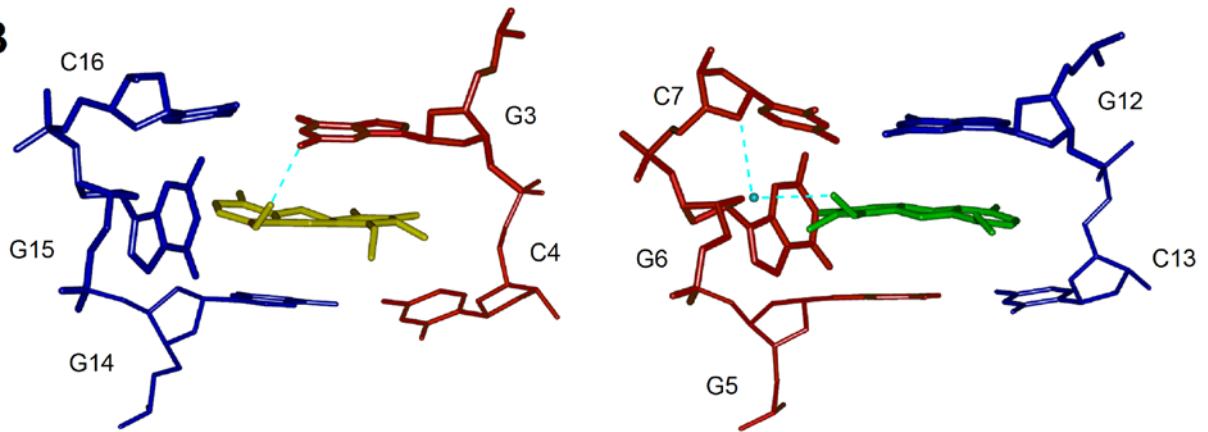


Figure S4

A



B



C

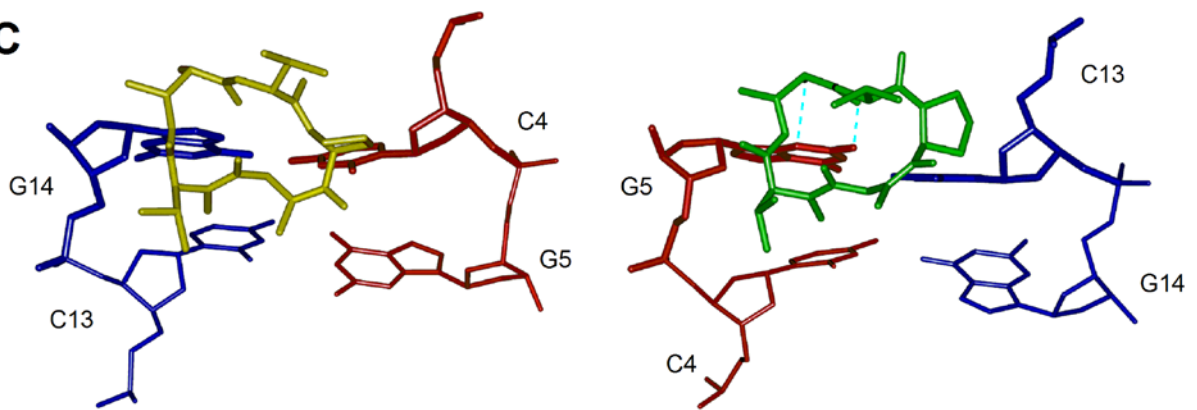
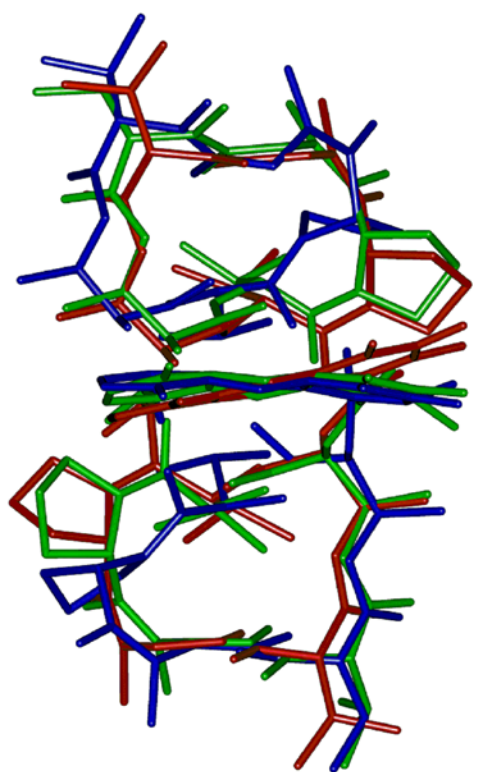
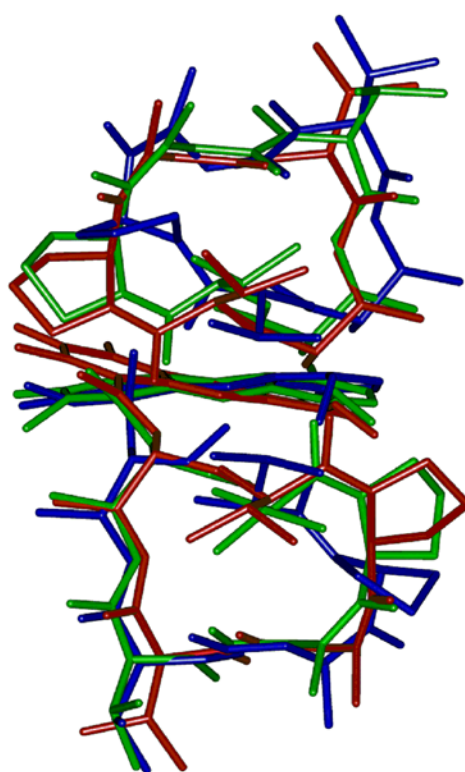


Figure S5



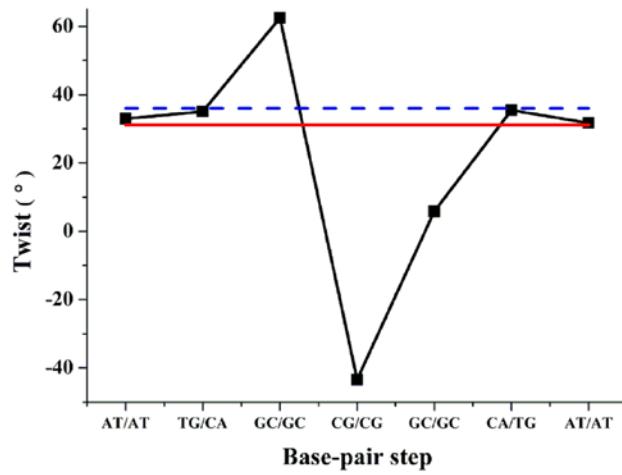
(Front view)



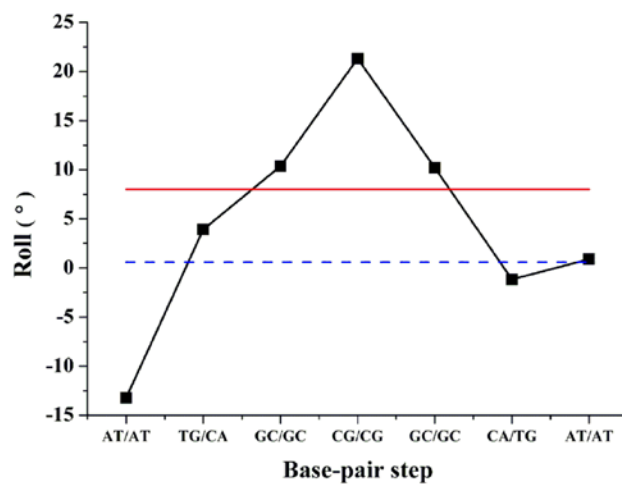
(Back view)

Figure S6

A.



B.



C.

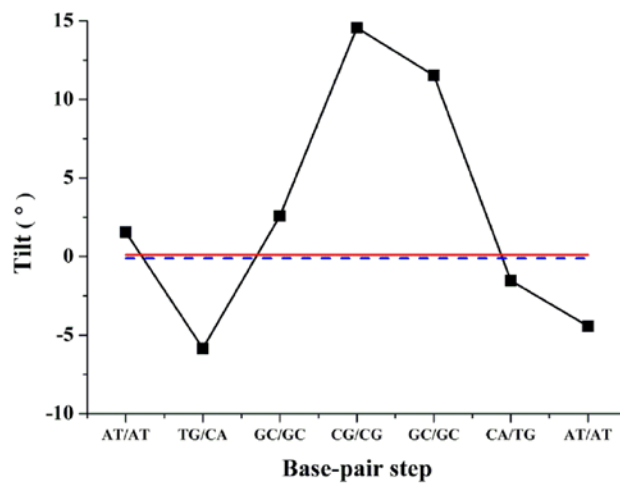
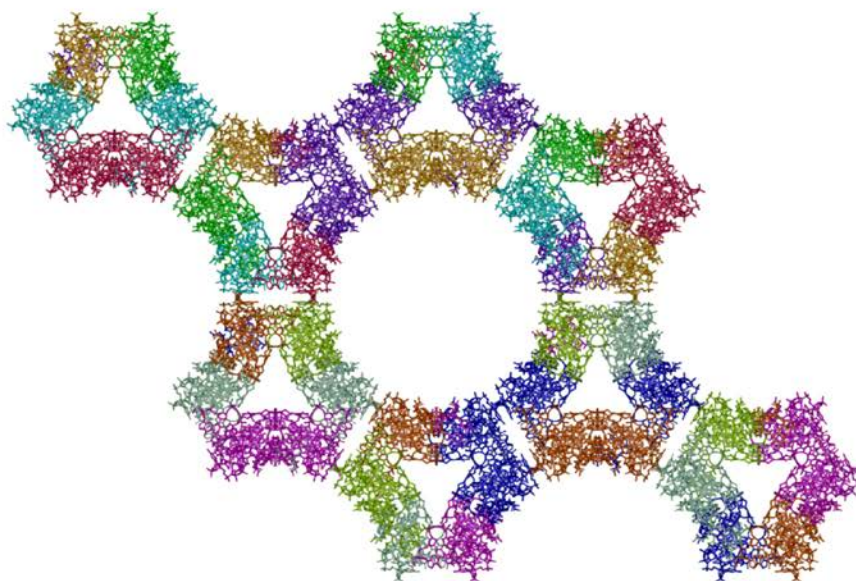


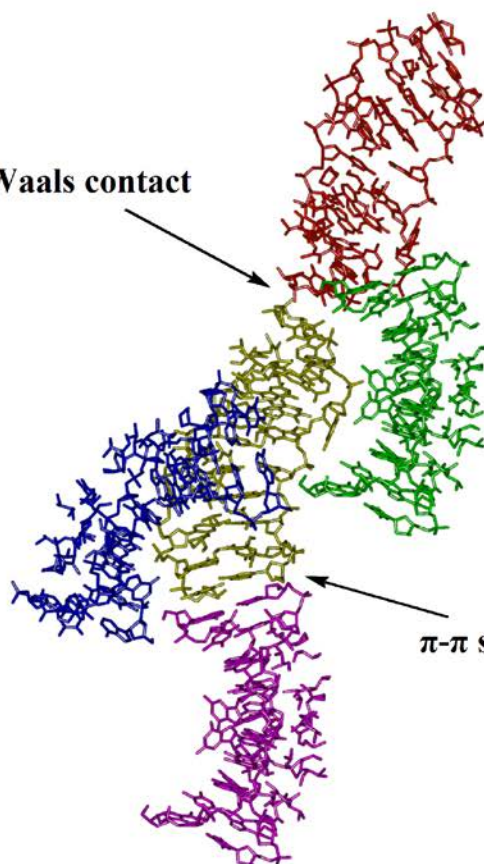
Figure S7

A.



B.

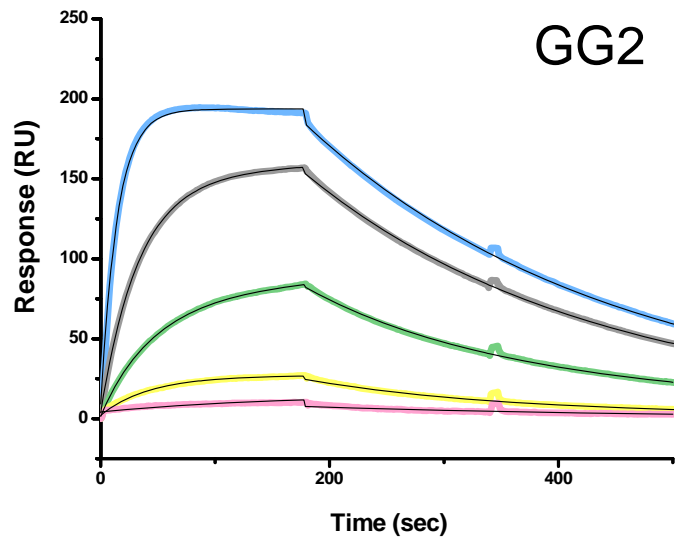
Van der Waals contact



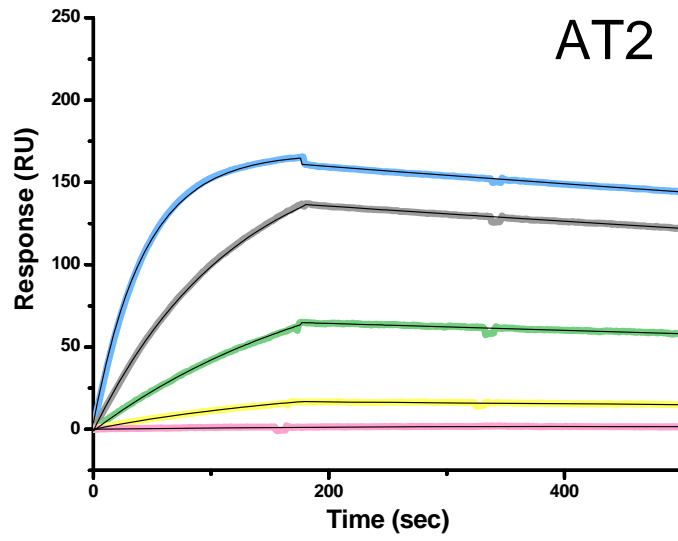
π - π stacking interaction

Figure S8

A.



B.



C.

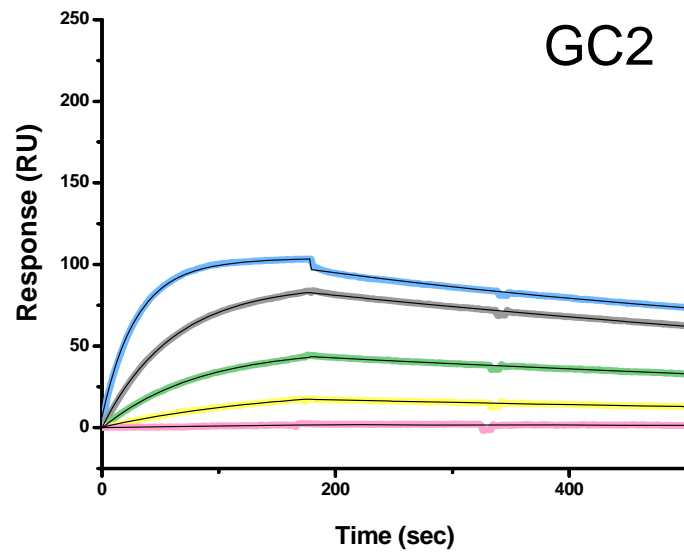


Figure S9

